

# Premelting Crystalline Relaxations and Phase Transitions in Nylon 6 and 6,6

N. S. Murthy,\* S. A. Curran, S. M. Aharoni, and H. Minor

Research and Technology, Allied-Signal, Inc., Morristown, New Jersey 07962

Received October 25, 1990; Revised Manuscript Received December 19, 1990

**ABSTRACT:** Variable-temperature XRD and NMR measurements show that nylon 6 (N6) undergoes crystalline relaxations between the glass transition temperature and the melting point. These relaxations bring about a crystalline transition between 80 and 170 °C from a monoclinic structure to a new crystalline structure, which is also most likely monoclinic. We thus demonstrate, for the first time, the presence of a Brill transition in N6, a phenomena that has been extensively studied in nylon 6,6 (N6,6). In both N6 and N6,6, the integrity of the H-bonded sheets is maintained during this transition and up to the melting point. The low- and high-temperature crystalline phases coexist during this transformation in both polymers, and the transition from the low-temperature to the high-temperature phase is diffuse, occurring over a temperature range of ca. 100 °C. Accelerated structural changes observed in N6 upon annealing above 170 °C, and the maxima in shrinkage and shrinkage stresses observed at ~180 °C in N6 and N6,6, are attributed to the onset of relaxation processes which produce these observed transitions. The relaxation is attributed to small torsional relaxations of the methylene segments pinned by the amide moiety. The possible high-temperature structures resulting from such oscillations are discussed.

## Introduction

Semicrystalline polymers exhibit several relaxation phenomena due to the onset of mobility of the chain segments in the amorphous and the crystalline regions.<sup>1</sup> Changes in the physical properties of the polymers that occur during these relaxation processes are of practical importance. For instance, it was shown by Aharoni and Sibilia<sup>2,3</sup> that many semicrystalline polymers can be extruded in the solid state at temperatures above a crystalline relaxation ( $\alpha_c$ ) temperature,  $T_{\alpha_c}$ ,<sup>1,4</sup> and below the melting point  $T_m$ . Solid-state extrusion is not feasible below  $T_{\alpha_c}$ , indicating that exceeding the glass transition temperature,  $T_g$ , alone is not sufficient. The  $\alpha_c$  transitions are manifested by abrupt increases in the thermal expansion coefficients,<sup>5</sup> drop in modulus,<sup>1</sup> and are accompanied by a weakening of the intracrystalline interactions.<sup>2,3</sup> The  $\alpha_c$  transitions are not first-order endothermic transitions, and, unlike the mesophasic transitions, the polymers do not flow spontaneously in the interval  $T_{\alpha_c} < T < T_m$ .

Claims that nylon 6 (N6) and nylon 6,6 (N6,6) can be extruded in the solid state at temperatures substantially below  $T_m$  have appeared in the literature.<sup>6,7</sup> Solid-state extrudability was marginal at best and hence was not pursued.<sup>2,3</sup> The crystalline transitions in N6 and N6,6 are apparently small and diffuse. Nevertheless, the changes in the structure, morphology, and properties in N6 and N6,6 annealed near these transition temperatures, i.e., between  $T_g$  and  $T_m$ , can be large.<sup>8-12</sup> It has been shown by X-ray diffraction (XRD),<sup>13,14</sup> differential scanning calorimetry (DSC),<sup>15</sup> and nuclear magnetic resonance (NMR)<sup>14</sup> that N6,6 undergoes a structural transformation between  $T_g$  and  $T_m$ , which is sometimes called the Brill transition. We will here report a similar transition in N6.

The crystalline transitions in N6 and N6,6 to be discussed here are similar to but not identical with the  $\alpha_c$  transitions commonly reported in the literature. The transitions in N6 and N6,6 occur over a broad range of temperatures, the interchain interactions within the crystalline regions are not markedly different on either side of the transition, and it has not been observed in a DSC scan of N6 but is sometimes observed in N6,6. For reasons given later (see the Discussion section), we shall

refer to the crystalline transition in both N6 and N6,6 as the  $\alpha_c$  transition. Variable-temperature XRD and spectroscopic measurements can provide definitive information on the structural origins of the endotherms associated with these  $\alpha_c$  transitions. In this paper we discuss our variable-temperature XRD data obtained from N6 and N6,6 and variable-temperature solid-state NMR data from N6 and present the evidence for a new crystalline phase in N6 above 170 °C. The nature of the segmental motions responsible for the onset of the crystalline transitions in N6 and N6,6 will be discussed.

## Experimental Section

N6 from Allied-Signal (Type 8207; viscosity of a 11% (w/v) formic acid solution, i.e.; formic acid viscosity or FAV ~ 70;  $M_n$  ~ 21 000 and  $M_w/M_n$  ~ 2) and N6,6 from Du Pont (Zytel 101; FAV ~ 50;  $M_n$  = 18 000–20 000) were used. X-ray diffraction scans were obtained by counting for 5 s at each 0.1° step ( $\theta/2\theta$  scan) on a Philips diffractometer in the parafocus geometry using copper radiation and a diffracted beam monochromator. An Anton-Paar variable-temperature attachment was used to heat the sample to the desired temperature. In this attachment, the sample is placed on a copper block whose temperature is electronically controlled. A thin layer (100  $\mu$ m) of finely powdered sample was used to reduce the thermal gradient across the thickness of the sample. A few particles of CaF<sub>2</sub> were added to the sample, and its diffraction peak at  $2\theta = 28.7^\circ$  was monitored to ensure that the observed shifts in the diffraction spacings are not due to artifacts such as thermal expansion of the copper block. Corrections due to thermal expansion of the copper block were found to be not necessary for our analysis. The polymer was first melted and then slowly cooled to room temperature in vacuo on the copper heating block so as to obtain a good thermal contact between the polymer and the heating block and also to obtain the  $\alpha$ -crystalline form. The sample was then heated gradually to the desired temperature in vacuo and held there for about 5 min before commencing the data collection. The diffraction spacings were calculated from the peak maxima, and the scans were profile fitted by using a modified version of the program SHADOW.<sup>16</sup>

Solid-state <sup>13</sup>C NMR spectra were acquired at 75.3 MHz on a Chemagnetics CMX-300 spectrometer. All spectra were acquired by 3.5 KHz magic angle spinning (MAS) to remove chemical shift anisotropy effects. The magic angle was set within 0.1° using the spinning side bands in a <sup>79</sup>Br spectrum of KBr. Data were acquired via cross-polarization (CP) and Bloch decay (BD), which enhance the rigid and mobile fractions, respectively.

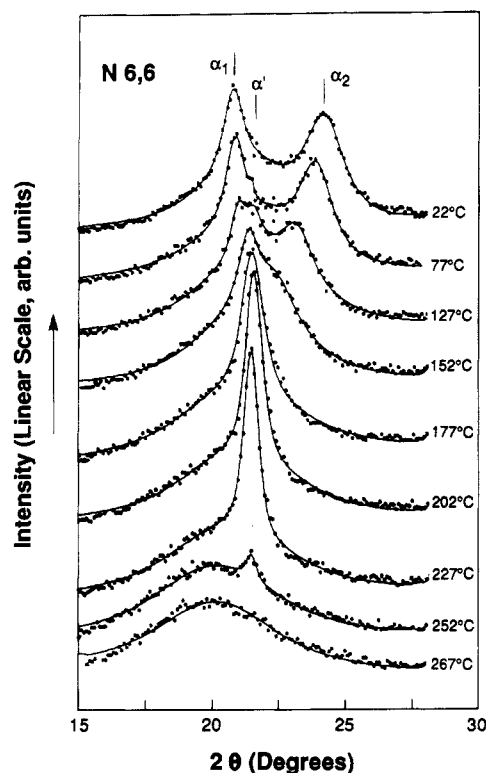


**Figure 1.** X-ray diffraction scans obtained at various temperatures (as indicated next to each curve) from N6,6. The filled circles are the observed data points, and the full line through these points is derived from profile analysis and is the sum of the various component peaks as shown in Figure 2a.

A 5- $\mu$ s 90° pulse was used in both CP and BD experiments. CP/MAS spectra were obtained by using 900- $\mu$ s contact times and a 2-s recycle time. BD/MAS spectra were obtained by using 10-s recycle delays to allow complete recovery of the amorphous polarization, based on inversion recovery measurements of spin-lattice relaxation times of the crystalline phase ( $T_{1\rho}$ ) of N6. A uniform temperature throughout the sample was difficult to achieve because of the low thermal conductivity of the zirconia rotor and the sample itself. Consequently, all samples were equilibrated at each temperature for ca. 4 h under nitrogen before acquiring the data. Chemical shifts are externally referenced to tetramethylsilane ( $^{13}\text{C}$ , 0 ppm) by using the methyl carbons of hexamethylbenzene at 17.4 ppm as an internal standard. The chemical shift reference was tested at room temperature before and after data acquisition. As one would expect for superconducting magnets, there was no appreciable change in  $H_0$ .

## Results

A series of profile-fitted X-ray diffraction (XRD) scans of N6,6 obtained from room temperature to melt are shown in Figure 1, and an example of the profile analysis using the scan at 127 °C is shown in Figure 2a. These results are similar to those reported in the paper by Hirschinger et al.<sup>14</sup> The XRD scans in Figure 1 reflect the substantial changes in the structure as the sample is heated to the melt. In the room temperature (22 °C) scan, there are two crystalline reflections at  $2\theta = 20.8^\circ$  ( $\alpha_1$ ) and  $24.3^\circ$  ( $\alpha_2$ ). A new peak at  $2\theta = 21.5^\circ$  ( $\alpha'$ ) appears at ca. 100 °C. The intensity of this new peak gradually increases with temperature with a concomitant decrease in the intensities of the two room-temperature peaks  $\alpha_1$  and  $\alpha_2$  as shown in Figure 3. With the counting statistics of the data in Figure 1, it is difficult to decide whether the new peak is present at temperatures as low as 80 °C, and hence the 80 °C point shown in Figure 3 may be questionable. The  $\alpha'$  peak is the only crystalline peak present at and above 170 °C; its intensity remains high and constant over the temperature

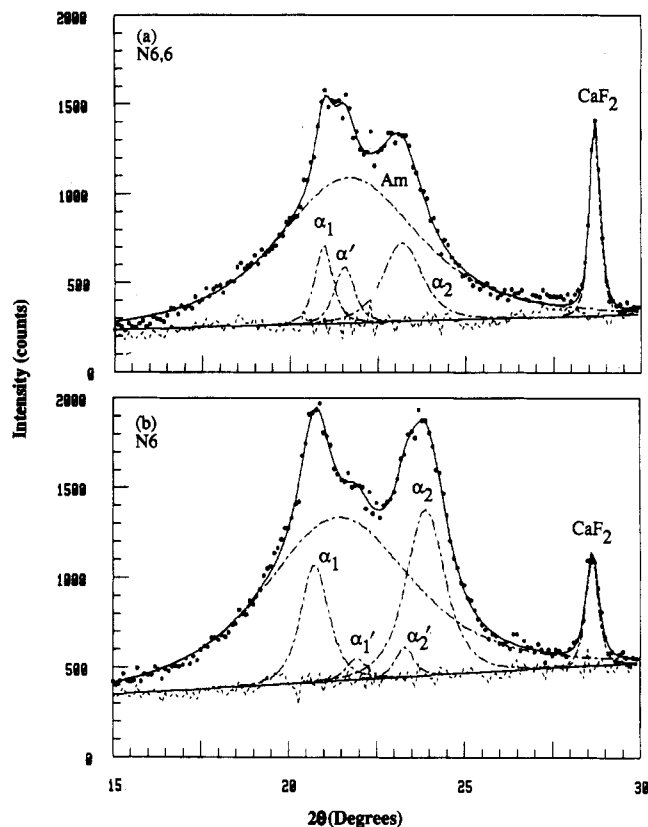


**Figure 2.** Examples of profile analysis of the diffraction scans from (a) N6,6 at 127 °C and (b) N6 at 77 °C. These scans were chosen so as to illustrate the coexistence of both the low- and high-temperature phases. The dots are the observed points, peaks shown in broken curves are the resolved components, the full curves are the sum of the components (this should overlap the observed data points), and the broken lines above and below the base line (shown by full line) represent the difference between the observed intensities and the calculated curves.

range of 170–230 °C, and it disappears at 260 °C ( $T_m$ ) in the molten polymer. The changes in the d-spacings and the intensities are plotted in Figure 3.

Profile-fitted XRD scans at various temperatures for N6 are shown in Figure 4, and an example of the profile analysis using the scan at 77 °C is shown in Figure 2b. Two crystalline peaks at  $2\theta = 20.7^\circ$  and  $24.3^\circ$  present in the room-temperature (22 °C) scan are due to the  $\alpha$  crystalline form of N6 and are labeled  $\alpha_1$  and  $\alpha_2$ , respectively. A new pair of peaks at  $2\theta = 22^\circ$  ( $\alpha'_1$ ) and  $23^\circ$  ( $\alpha'_2$ ) appear at ca. 80 °C. The intensities of the new peaks gradually increase with temperature, and, as in N6,6, there is a simultaneous decrease in the intensities of the  $\alpha_1$  and  $\alpha_2$  crystalline peaks of the room-temperature phase of N6 as shown in Figure 5. However, while the high-temperature phase of N6,6 showed a single peak at  $2\theta = 21.5^\circ$ , in N6 the peak at  $2\theta = 23\text{--}24^\circ$  persists along with the  $22^\circ$  peak even in scans obtained prior to melting ( $\sim 10^\circ$  below  $T_m$ ). Between 170 °C and the melting temperature of 220 °C, the new pair of peaks ( $\alpha'_1$  and  $\alpha'_2$ ) shifts to  $21.5^\circ$  and  $22.7^\circ$ , respectively, but their intensities remain virtually unchanged until they disappear in the molten polymer at 220 °C ( $T_m$ ). The changes in the d-spacings and the intensity of the reflections as a function of temperature are plotted in Figure 5.

A series of BD/MAS N6 spectra at various temperatures between room temperature and the melt are shown in Figure 6. In these spectra, the response from the rigid-chain segments in the crystalline phase is selectively suppressed because of their extremely long spin-lattice relaxation times. As expected, the amorphous peaks

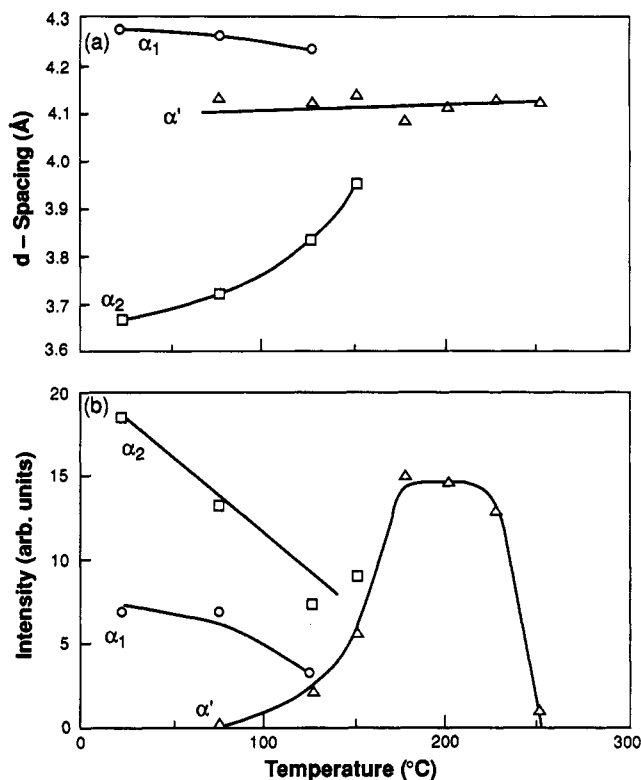


**Figure 3.** Plot of the changes in (a) the diffraction spacings and (b) the intensities of the Bragg reflection as a function of temperature in N6,6. A full line has been drawn (free-hand) through the data points to emphasize the transition.

steadily become sharper with an increase in temperature.

The solid-state NMR CP/MAS spectra of N6 obtained at various temperatures from room temperature into the melt are shown in Figure 7. A BD/MAS spectrum is included in this figure to show the locations of the amorphous N6 peaks. In contrast to the BD spectra, the response of the amorphous peaks is suppressed in a CP spectra. This effect becomes more pronounced with an increase in the amorphous mobility. Thus, with an increase in temperature, the amorphous intensity in a CP spectrum steadily decreases until it disappears completely at  $\sim 75$  °C.

As the temperature increases above 75 °C, new peaks begin to appear in the spectrum with chemical shifts close to, but not the same as, those of the amorphous or the  $\gamma$  peaks of N6 (Table I).<sup>17</sup> These CP peaks are broader than the amorphous peaks in the BD spectrum; they increase in intensity up to 180 °C and then disappear in the melt. The increase in the fraction of the crystalline intensity in these new peaks with temperature is shown in Figure 8. This fraction reaches a maximum of  $\sim 10\%$  of the crystalline phase of N6.

## Discussion

The XRD data for N6,6 in Figure 3 are a quantitative representation of the triclinic to triclinic transition in N6,6 between ca. 80 and 170 °C, the Brill transition.<sup>13,14</sup> To a first approximation, the  $\alpha_1$  peak ( $2\theta \approx 21^\circ$ ) arises from the distance between hydrogen-bonded chains, and the  $\alpha_2$  peak ( $2\theta \approx 23^\circ$ ) arises from the separation of the hydrogen-bonded sheets. The absence of the  $\alpha_2$  peak at temperatures  $> 170$  °C (above the Brill transition) has been taken to imply that the H-bonded sheets are replaced at higher temperatures by a random distribution of H bonds around the chain axis. However, Hirschinger et al.<sup>14</sup> have recently shown from their  $^2\text{H}$  NMR studies that the mobility of the

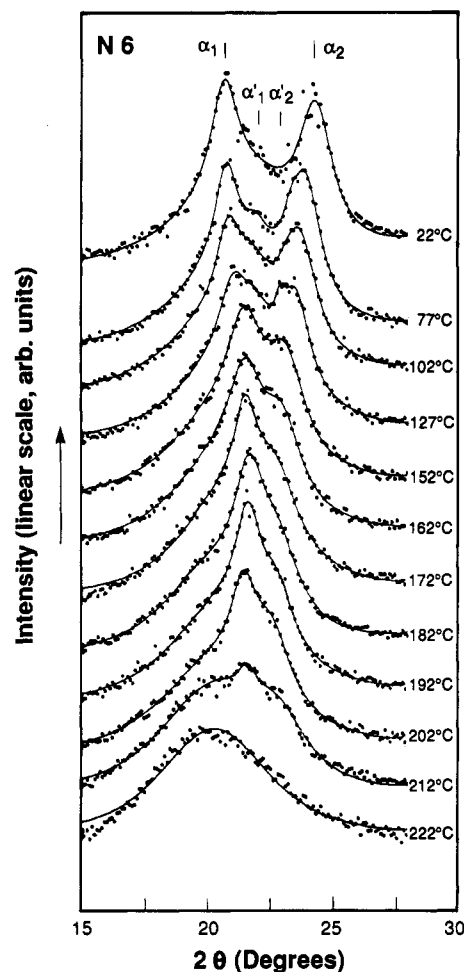


**Figure 4.** X-ray diffraction scans from N6 obtained at temperatures shown next to each of the scans. The filled circles are the observed data points, and the full line through these points is derived from profile analysis and is the sum of the various component peaks as shown in Figure 2b.

amide moiety in the crystalline phase is minimal and that the H-bonded sheet structure is maintained even near the melting temperature of N6,6. Since the Brill transition has the connotation of the formation of a pseudohexagonal phase, the term  $\alpha_c$  transition, which we have adopted here, is applicable to all instances in which there is a structural transformation of the crystal lattice and hence is to be preferred.

Itoh, in his X-ray measurements on biaxially oriented nylon films, found a continuous structural change in N6 and N6,6 with no evidence for a Brill transition.<sup>18</sup> We speculate that, in biaxially oriented films, the amorphous phase and the crystalline regions are constrained differently from that in unoriented or uniaxially oriented specimens. These differences might preclude the nearly hexagonal packing of the polymer chains and hence the occurrence of Brill transition.

The XRD data from N6 (Figures 4 and 5) show that, at ca. 160 °C (which is about the same as the Brill transition in N6,6), the pair of peaks at  $2\theta = 20.5^\circ$  and  $24^\circ$  is replaced by a new pair of peaks at  $21.5^\circ$  and  $23^\circ$ . This is indicative of a structural transformation from one monoclinic lattice to a different crystalline (probably also monoclinic) lattice. Thus, N6 undergoes a structural transition similar to that in N6,6. This is the first reported observation of a Brill transition in N6.

There are significant similarities and differences in the crystalline transition observed in N6 and N6,6 with an increase in temperature. The transition in both the poly-



**Table II**  
Spin-Lattice Relaxation for Carbons ( $T_{1\rho}$ ) in the  $\alpha'$  Phase at 180 °C

time, s	carbons (see Table I)				
	C <sub>2</sub>	C <sub>3</sub>	C <sub>4</sub>	C <sub>5</sub>	C <sub>6</sub>
	85	65	69	69	79

terplanar spacing of 4.1 Å, and N6 has two distinct interplanar spacings of 3.9 and 4.1 Å. Thus, the distance between the planes of H-bonded chains and the H-bonded sheets in the high-temperature phase is about the same for N6,6 but is different for N6. While the high-temperature phase of N6 resembles the structure at room temperature, that of N6,6 does not. The absence of a single sharp crystalline peak in N6 clearly suggests that, as in N6,6,<sup>14</sup> the integrity of the H bonds is maintained past this transition temperature, up until the polymer melts at 220 °C.

The broad  $\alpha_c$  transition (from ~80 to ~170 °C) observed in N6 and N6,6 can be attributed to crystallites of varying stabilities. It could also be due to H bonding in polyamides, since polymers that do not have H bonds exhibit a sharp  $\alpha_c$  transition.<sup>3</sup> The H bonds also account for the large heat and entropy of fusion in both N6 and N6,6 relative to the non-H-bonded polymers. As the temperature is increased, the contributions of the H bonds and the van der Waals interactions to the energy minimum are expected to change at different rates. The observation of new structures shows that as the interchain distances between the H-bonded and non-H-bonded chains are varied, there exists more than one pair of distances at which the sum of the two contributions reaches a minimum. The secondary structures at these local minima can be stable over a limited range of temperature, or other similar external variables, such as stress.<sup>19</sup>

The CP NMR spectra of N6 show that at room temperature the polymer chains in the crystalline regions are in the fully extended, mostly trans conformation ( $\alpha$  form). New peaks begin to appear at 100 °C in the CP spectrum (Figure 7). Since these new NMR peaks are not present in the BD spectrum and are not present in the spectra obtained from molten N6, we conclude that these new peaks are not from amorphous chain segments. These new peaks could be due either to a new crystalline phase or to a new chemical shift from constrained amorphous chain segments.<sup>20</sup> Our data indicate that the new chemical shifts are indeed due to a crystalline phase. The chemical shifts of C<sub>2</sub> and C<sub>6</sub> carbons are close to that of amorphous N6, but those of C<sub>3</sub>, C<sub>4</sub>, and C<sub>5</sub> are different from that of amorphous N6. The BD experiments, which are selective to rapidly relaxing spins, show evidence for only the room-temperature amorphous N6. New peaks expected of constrained amorphous segments which would have relatively short  $T_{1\rho}$ 's are not present in the high-temperature BD spectra (Figure 6). Finally, we measured the carbon spin-lattice relaxation times ( $T_{1\rho}$ ) at 180 °C using the method of Torchia<sup>21</sup> for slowly relaxing spins. The peaks that we have assigned to the  $\alpha'$  phase have long relaxation times (Table II) and are characteristic of the rigid crystalline phase rather than of the amorphous phase. These conclusions are consistent with the appearance of new crystalline reflections in the XRD scans at the same temperature at which the new chemical shifts are observed in the NMR spectra (Figures 4 and 6).

The chemical shifts of these new peaks are different from both the  $\alpha$  and the  $\gamma$  nylon 6 and are consistent with the conversion of a fraction (10%) of the C-C bonds in the crystalline regions from trans to gauche configuration

without loss of the crystal integrity. Thus, an increase in the intensity of the new peak with temperature (Figure 8) could indicate that the fraction of gauche C-C bonds in the  $\alpha$  crystalline regions increases with temperature. In other words, the extent of configurational disorder in the  $\alpha$  crystallites increases with temperature during the Brill transition, without melting or converting to amorphous N6. The motions associated with the appearance of gauche conformations may be torsional oscillations of the methylene segments over a small angular range. Such motions are similar to the  $\alpha_c$  relaxation observed in many other polymers,<sup>1-4</sup> except that the segments are pinned by the H-bonded amide groups in N6 and N6,6.

The XRD data (Figures 4 and 5) show that the room-temperature  $\alpha$  phase is replaced by the high-temperature  $\alpha'$  phase at ca. 180 °C, but NMR data (Figure 7) show peaks attributable to the  $\alpha$  crystalline phase (C<sub>2</sub> and C<sub>6</sub>) even at 180 °C. We suggest these peaks are due to chains that maintain the  $\alpha$ -like conformation even in the high-temperature  $\alpha'$  phase. This interpretation is consistent with the observation that the new NMR peaks represent an increased rotational mobility about the chain axis of a fraction (~10%) of the carbons that change from trans to gauche in the crystalline chain segments. Such retention of the trans conformation is most evident in the carbons next to the amide moiety. These results (from chemical shift measurements) are in agreement with the conclusions of Hirschinger et al.<sup>14</sup> (from relaxation measurements) that amide N-D groups undergo very little rotational motion.

The apparent inconsistencies between the XRD and NMR results can be further reconciled in a model in which the high-temperature phase is created by a lateral shift of adjacent hydrogen-bonded sheets; this does not entail a major conformational change along the chain axis. It is most likely that a change from trans to gauche of about 1 in 10 carbons, and the accompanying increase in the mobility of the chains, is sufficient to alter the strength of the van der Waals interactions between the H-bonded sheets. This may bring about the observed transformation of the crystal structure. Using 1.27, 1.25, 1.21, and 1.09 Å for the chain-axis contribution of the CH<sub>2</sub>-CH<sub>2</sub>, CH<sub>2</sub>-CO, CH<sub>2</sub>-NH, and CO-NH bonds, respectively, we obtain a chain-axis repeat of 17.26 Å for the extended chain conformation. If we substitute one gauche conformation in each crystallographic repeat (10% of the methylene carbons), then using a chain-axis length of 0.4 Å for the gauche bond,<sup>22</sup> we calculate a chain-axis repeat of 16.88 Å. These values are in excellent agreement with the values 17.25 Å at 22 °C and 16.87 Å at 200 °C observed by Itoh.<sup>18</sup> We have no evidence for the pleated  $\alpha$  sheets proposed by Stepaniak et al.<sup>23</sup> in which the hydrogen-bonded antiparallel chains have the conformation found in the  $\gamma$  structure so that the chain-axis repeat is 16.8 Å.

The distance between the hydrogen-bonded chains in N6 is significantly shorter in the high-temperature phase than in the room-temperature phase. This finding is in agreement with the observation that the hydrogen bonds are stronger in the less dense phases of N6, such as the amorphous and the  $\gamma$  phases.<sup>24</sup> Because of lack of sufficient data, it is difficult to calculate the unit cell parameters of the high-temperature phase. Let us assume that the unit cell of the high-temperature phase of N6 is similar to its room-temperature monoclinic unit cell. Then,  $d(\alpha'_1) = (a \sin \beta)/2$  and  $d(\alpha'_2) = (c \sin \beta)/2$ ;  $\beta$  being the monoclinic angle, and  $b$  the chain axis. Thus, it is possible to calculate the ratio  $c/a$  of the unit-cell dimensions in chain-axis projection without knowing  $\beta$ .<sup>25,26</sup> This ratio for the high-temperature phase varies between 0.94 (at 162 °C) and

0.95 (at 212 °C) compared to 0.84 in a typical annealed, room-temperature sample of  $\alpha$  N6. This suggests that the crystalline phase between 170 and 220 °C in N6 might be a metastable phase.<sup>19,26</sup> The new crystalline peaks observed in the NMR spectra show that the conformation of the chains in this crystalline phase can be distinguished from both the  $\alpha$  and the  $\gamma$  crystalline phases. Additional experiments are necessary to confirm that the new phase is indeed a metastable phase.

The structural transformations discussed above can be helpful in understanding the reported large changes in the morphology and mechanical properties observed in N6 and N6,6 samples annealed above  $\sim 160$  °C. XRD from annealed fibers<sup>10-12</sup> show that many of the structural parameters in N6 begin to change significantly (increase in the lamellar spacing, crystallite size, and density and decrease in the interplanar spacings in the crystalline lamellae) at ca. 170 °C in dry atmosphere. Matyi and Crist<sup>9</sup> have shown that tensile strength decreases abruptly when N6 is annealed above 170 °C (in silicone oil for 1 min), and this is accompanied by an increase in the shrinkage of the fiber. Ribnick<sup>8</sup> observed a similar maximum in thermal shrinkage in N6,6 at  $\sim 180$  °C. Takayanagi<sup>1,4</sup> showed a substantial shoulder in the mechanical loss,  $\tan \delta$ , at ca. 160 °C for highly purified N6 in its  $\alpha$  crystalline modification, indicating a crystalline transition that he termed  $\alpha_c$ . Finally, Dennis and Buchanan<sup>27</sup> observed that the shrinkage stresses in their thermal stress analysis (isometric heating) experiments go through a maximum at  $\sim 160$  °C, in addition to one at  $\sim 90$  °C; while the 90 °C transition is due to the increase in the mobility of the chain segments in the amorphous regions above the glass transition temperature, no definitive mechanism was proposed for the 170 °C transition.

Many explanations, such as crystalline reorganization, melting of imperfect or small crystals, and recrystallization, have been suggested<sup>27</sup> to account for the changes occurring at ca. 170 °C. Our data clearly suggest that these changes are due to enhanced mobility of the chains in the crystalline regions, which also bring about a transformation from one crystalline structure to another. The chains become more mobile at ca. 170 °C due to the onset of minor oscillations of the crystalline stems. In N6, these oscillations are consistent with conversion of up to 10% of the methylene carbons from trans to gauche. In N6,6, Hirschinger et al.<sup>14</sup> have shown from their <sup>2</sup>H NMR measurements on deuterated polymers that the mean librational amplitude of the C-D bonds increases at  $T_{\alpha_c}$ .

The enhanced mobility associated with the  $\alpha_c$  relaxation can give rise to maxima in shrinkage stresses and may account for the large changes in unit-cell dimensions, crystallite sizes, lamellar spacings, and macroscopic dimensions in N6 and N6,6 annealed at temperatures above ca. 170 °C.

**Acknowledgment.** We thank R. D. Sedgwick, A. C. Reimschuessel, and A. J. Signorelli for reviewing the manuscript and for their helpful comments.

## References and Notes

- (1) McCrum, N. G.; Read, B. E.; Williams, G. *Anelastic and Dielectric Effects in Polymeric Solids*; Wiley: London, 1967; pp 478-483.
- (2) Aharoni, S. M.; Sibilia, J. P. *J. Appl. Polym. Sci.* **1979**, *23*, 133.
- (3) Aharoni, S. M.; Sibilia, J. P. *Polym. Eng. Sci.* **1979**, *19*, 450.
- (4) Takayanagi, M. *Mem. Fac. Eng., Kyushu Univ.* **1963**, *23*, 41; personal communication, July 1978.
- (5) Enns, J. B.; Simha, R. *J. Macromol. Sci., Phys.* **1977**, *B13*, 11 and 25.
- (6) Murayama, S.; Imada, K.; Takayanagi, M. *Int. J. Polym. Mater.* **1973**, *2*, 125.
- (7) Buckley, A.; Long, H. A. *Polym. Eng. Sci.* **1969**, *9*, 115.
- (8) Ribnick, A. *Textile Res. J.* **1969**, *39*, 428.
- (9) Matyi, R. J.; Cryst, B., Jr. *J. Polym. Sci., Polym. Phys. Ed.* **1978**, *16*, 1329.
- (10) Park, J. B.; Devries, K. L.; Statton, W. O. *J. Macromol. Sci., Phys.* **1978**, *B15*, 229.
- (11) Baldrian, J.; Pelzbauer, Z. *J. Polym. Sci., Part C* **1972**, *No. 38*, 289.
- (12) Murthy, N. S.; Minor, H.; Latif, R. A. *J. Macromol. Sci., Phys.* **1987**, *B26*, 427.
- (13) Brill, R. *J. Prakt. Chem.* **1942**, *161*, 49.
- (14) Hirschinger, J.; Miura, H.; Gardner, K. H.; English, A. D. *Macromolecules* **1990**, *23*, 2153.
- (15) Starkweather, H. W., Jr. *Macromolecules* **1989**, *22*, 2000 and references therein.
- (16) Murthy, N. S.; Minor, H. *Polymer* **1990**, *31*, 996.
- (17) Hatfield, G. R.; Glans, J. H.; Hammond, W. B. *Macromolecules* **1990**, *23*, 1654.
- (18) Itoh, T. *Jpn. J. Appl. Phys.* **1976**, *15*, 2295.
- (19) Murthy, N. S. *Polym. Commun.*, **1991**.
- (20) Miura, H.; Hirschinger, J.; English, A. D. *Macromolecules* **1990**, *23*, 2169.
- (21) Torchia, D. A. *J. Magn. Reson.* **1978**, *30*, 613.
- (22) Aharoni, S. M.; Correale, S. T.; Hammond, W. B.; Hatfield, G. R.; Murthy, N. S. *Macromolecules* **1989**, *22*, 1137.
- (23) Stepaniak, R. F.; Garton, A.; Carlsson, D. J.; Wiles, D. M. *J. Polym. Sci., Polym. Phys. Ed.* **1979**, *17*, 987.
- (24) Murthy, N. S.; Stamm, M.; Sibilia, J. P.; Krimm, S. *Macromolecules* **1989**, *22*, 1261.
- (25) Salem, D. R.; Weigmann, H.-D. *Polym. Commun.* **1989**, *30*, 336.
- (26) Murthy, N. S.; Minor, H. *Polym. Commun.*, **1991**.
- (27) Dennis, L. A.; Buchanan, D. R. *Textile Res. J.* **1987**, *57*, 625.